Lab on a Chip
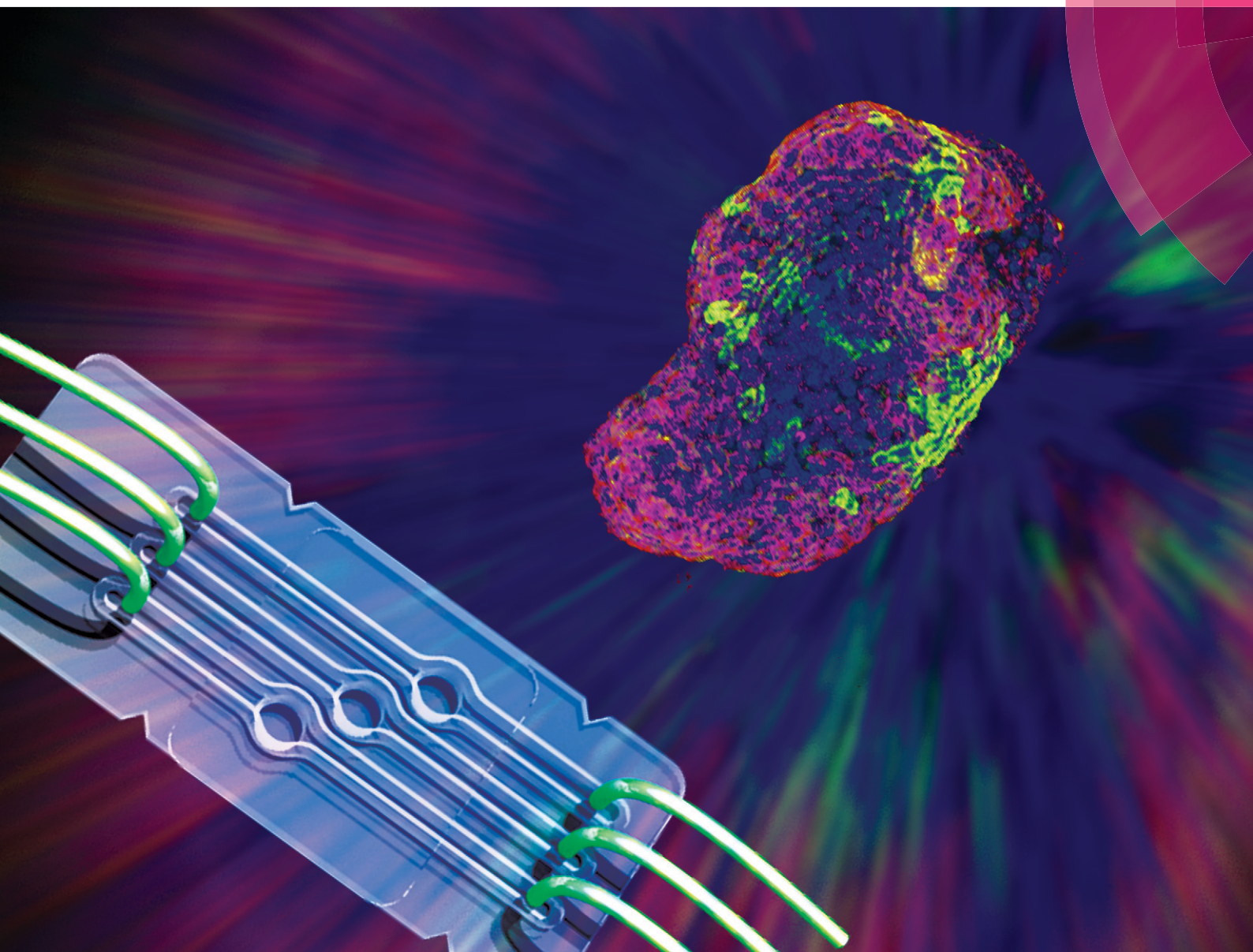
Miniaturisation for chemistry, physics, biology, materials science and bioengineering

rsc.li/loc

ROYAL SOCIETY
OF CHEMISTRY

PAPER
Ashutosh Agarwal *et al.*
Resealable, optically accessible, PDMS-free fluidic platform for *ex vivo* interrogation of pancreatic islets

Resealable, optically accessible, PDMS-free fluidic platform for *ex vivo* interrogation of pancreatic islets†

Giovanni Lenguito,[a] Deborah Chaimov,[b] Jonathan R. Weitz,[c]
Rayner Rodriguez-Diaz,[c] Siddarth A. K. Rawal,[a] Alejandro Tamayo-Garcia,[d]
Alejandro Caicedo,[c] Cherie L. Stabler,[b] Peter Buchwald[de] and Ashutosh Agarwal*[ad]

We report the design and fabrication of a robust fluidic platform built out of inert plastic materials and micromachined features that promote optimized convective fluid transport. The platform is tested for perfusion interrogation of rodent and human pancreatic islets, dynamic secretion of hormones, concomitant live-cell imaging, and optogenetic stimulation of genetically engineered islets. A coupled quantitative fluid dynamics computational model of glucose stimulated insulin secretion and fluid dynamics was first utilized to design device geometries that are optimal for complete perfusion of three-dimensional islets, effective collection of secreted insulin, and minimization of system volumes and associated delays. Fluidic devices were then fabricated through rapid prototyping techniques, such as micromilling and laser engraving, as two interlocking parts from materials that are non-absorbent and inert. Finally, the assembly was tested for performance using both rodent and human islets with multiple assays conducted in parallel, such as dynamic perfusion, staining and optogenetics on standard microscopes, as well as for integration with commercial perfusion machines. The optimized design of convective fluid flows, use of bio-inert and non-absorbent materials, reversible assembly, manual access for loading and unloading of islets, and straightforward integration with commercial imaging and fluid handling systems proved to be critical for perfusion assay, and particularly suited for time-resolved optogenetics studies.

Introduction

Islets of Langerhans are 50–500 μm diameter clusters of multiple cells (mainly α, β, δ, γ) within the pancreas. Each of these cell types are functionally interdependent, and responsible for different protein or hormone secretion.[1] While only the β cells are responsible for insulin secretion, islets are often considered the minimum functioning unit for controlled insulin release. Type 1 diabetes mellitus results from the autoimmune destruction of these insulin-secreting β cells and is one of the most common and costly chronic pediatric disease. Type 2 diabetes mellitus results from insulin deficiency and/or insulin resistance, and accounts for 90% of diabetes cases. Diabetes affects about 300 million people worldwide, and is expected to affect over 400 million by 2030.[1] In the US alone, the total estimated cost of diagnosed diabetes was $345 billion in 2012, an increase of 41% since 2007.[2]

The development of a robust tool for *ex vivo* evaluation of pancreatic islets is important and timely for a multitude of emerging thrust areas within diabetes research and therapy. First, clinical transplantation of islets is developing into a viable therapy for type 1 diabetes mellitus,[3] which makes it increasingly important to consistently and reliably assess the quality of isolated pancreatic islet cells. Since transplanted islets experience a dynamic stimulatory environment and secrete hormones in response to these ongoing stimuli, it is critical to test pre-transplant islets in devices that recreate dynamic sequential events[4] such as changes in glucose and other environmental inputs[5] rather than conventional static wells or plates. Second, sustainable sources of functional β cells are beginning to be derived from stem and precursor cell sources for similar regenerative medical applications.[6,7] Despite remarkable achievements, the inability to maintain islet function underlines the importance of bioengineering a pancreatic niche within fluidic microdevices to sustain cell maturation and test function over extended periods. Third, organs on chips are being developed to supplement high

a Department of Biomedical Engineering, Department of Pathology & Laboratory Medicine, University of Miami, Miami, FL 33136, USA.
E-mail: A.agarwal2@miami.edu; Fax: +1 305 243 6170; Tel: +1 305 243 8925
b Department of Biomedical Engineering, University of Florida, USA
c Department of Endo-Diabetes, University of Miami, USA
d Diabetes Research Institute, University of Miami, USA
e Department of Molecular and Cellular Pharmacology, University of Miami, USA
† Electronic supplementary information (ESI) available. See DOI: 10.1039/c6lc01504b

throughput screening methods and reduce the use of animal models for drug development in a more human relevant platform.[8,9] Development of *in vitro* models that test human islets in a dynamic and high throughput manner while enabling multiple assays for functional evaluation such as imaging[10–13] and collection of biochemical samples for insulin detection[14] would directly support this research area.[15] All too often, however, the sophistication of these devices discourages the widespread distribution and their use by the islet research community. Nonetheless, the ability to apply physiological perturbations and fluidically introduce pathological stressors, such as the effects of immune cells, makes these fluidic microdevices powerful tools for studying pathways for onset of diabetes,[16,17] discovering biomarkers of beta cell death,[18] and investigating strategies for the targeting and regeneration of functional beta cell mass.[19,20]

Commercially available perfusion systems (such as the PERI4-02™ from Biorep Inc., Miami, FL) offer clear advantages over static systems.[21] However, this confined system does not permit the engineering of the microenvironment or support parallel functionalities such as long-term culture or imaging. Further, these devices suffer from large system volumes and associated delays and are often cumbersome in terms of islet loading and retrieval. Microfluidic devices,[22,23] built with specialized soft photolithography techniques from transparent polydimethylsiloxane (PDMS) material, often leverage control over laminar fluid flow at the microscale and overcome many of those limitations.[9] However, many of the design features prevent broad adoption of those technologies by the scientific community. Among others, they include: (i) lack of manufacturing scalability due to reliance on clean room-based soft photolithography fabrication, (ii) unsuitability as drug testing platforms due to absorption of hydrophobic reagents and leaching of small molecules by PDMS, (iii) lack of standardized fluidic ports or industry compliant form factors, and (iv) restrictions in loading cell clusters due to permanent bonding of fluidic chips that necessitate islet loading through fluidic channels; and exposing them to shear stresses and making their recovery difficult.[24]

In this article, we present the design and fabrication of 3 well fluidic platform, called FP-3W that supports the dynamic testing of pancreatic islets for glucose-stimulated insulin secretion (GSIS) and concomitant live-cell imaging. The device geometry was optimized for effective perfusion using a validated first principle model of insulin secretion dynamics, coupled with a computational fluid dynamics model. The FP-3W was fabricated using rapid prototyping techniques and built from a bio-inert acrylic plastic material, with the capability for large scale production through injection molding. The device can be manually loaded and reversibly sealed using commercially available clamps, resulting in simple, yet robust, operation. We demonstrate the easy integration of the device with standard imaging and fluid handling platforms typically available in research laboratories. Finally, tests are conducted to detect light-induced somatostatin secretion in islets from transgenic mice whose delta cells

expressed the light sensitive ionic channel channelrhodopsin-2 (Chr2). Collection and detection of small levels of hormone in response to optogenetic stimulation serves as a powerful validation of the various design features of FP-3W: optimized fluid flow, reversible assembly, robust operation, optical access, and integration with imaging and fluid handling systems.

Design and fabrication

Computational fluid dynamics

The goal of this study was to design a geometry that could be manufactured with rapid prototyping techniques, such as laser engraving and micromachining, while effectively fulfilling the requirements of on-demand rapid assessment of islet functionality, such as dynamic GSIS, and eventually long-term culture of pancreatic islets. Specifically, GSIS consists of perfusing the islets with low (*e.g.*, 3–5 mM) then high stimulatory (*e.g.*, 11–28 mM) glucose solutions and measuring the corresponding insulin released over the experimental time period (*e.g.*, one hour). The fluid path plays an essential role in transporting the required stimulants to the islets without excessively stressing them, while concurrently clearing the secreted hormones without any unnecessary delay or accumulation in fluidic dead-zones. To optimize the geometry of the design, 2D computational fluid dynamics (CFD) simulation was coupled to a quantitative model of glucose-insulin dynamics based on the spatial distribution of the concentrations of glucose and oxygen.[25] A COMSOL framework that uses the finite element method was employed to integrate fluid mechanics, convective and diffusive mass transport, and reaction rates. The fluid mechanics was modeled with incompressible Navier–Stokes equations, no slip (zero velocity) boundary condition on solid surfaces, and no viscous stress (zero static pressure) at the outlet. No mass transport was set through the walls of the device. The influx of glucose and oxygen was set to be transported with the inlet velocity. Islet nutrient consumption and hormone secretion was modeled with a Hill-type sigmoid dependence on local concentration, while insulin release was modeled in a first and second phase, depending on the glucose time-gradient and its concentration, respectively.[26] At the outlet, insulin, glucose and oxygen were allowed to freely flow outward. Initial conditions on glucose flux, insulin production and oxygen consumption were fixed for the first minutes to contain computational residues and stabilize the calculation (that is why glucose flux is null at the beginning, Fig. 1B, and the insulin is gradually released at the beginning, Fig. 1C).

The device configuration was considered to be optimal if the islets experienced changes in perfused glucose in an efficient manner at all positions within the well, while being exposed to minimal shear stress. This was enforced through several geometrical features within the device (Fig. 1A). The well, 4 mm in width (diameter) and 1.5 mm in height, was designed to be similar to a standard 96-well plate in order to limit response delay due to excessive dead volume and allow
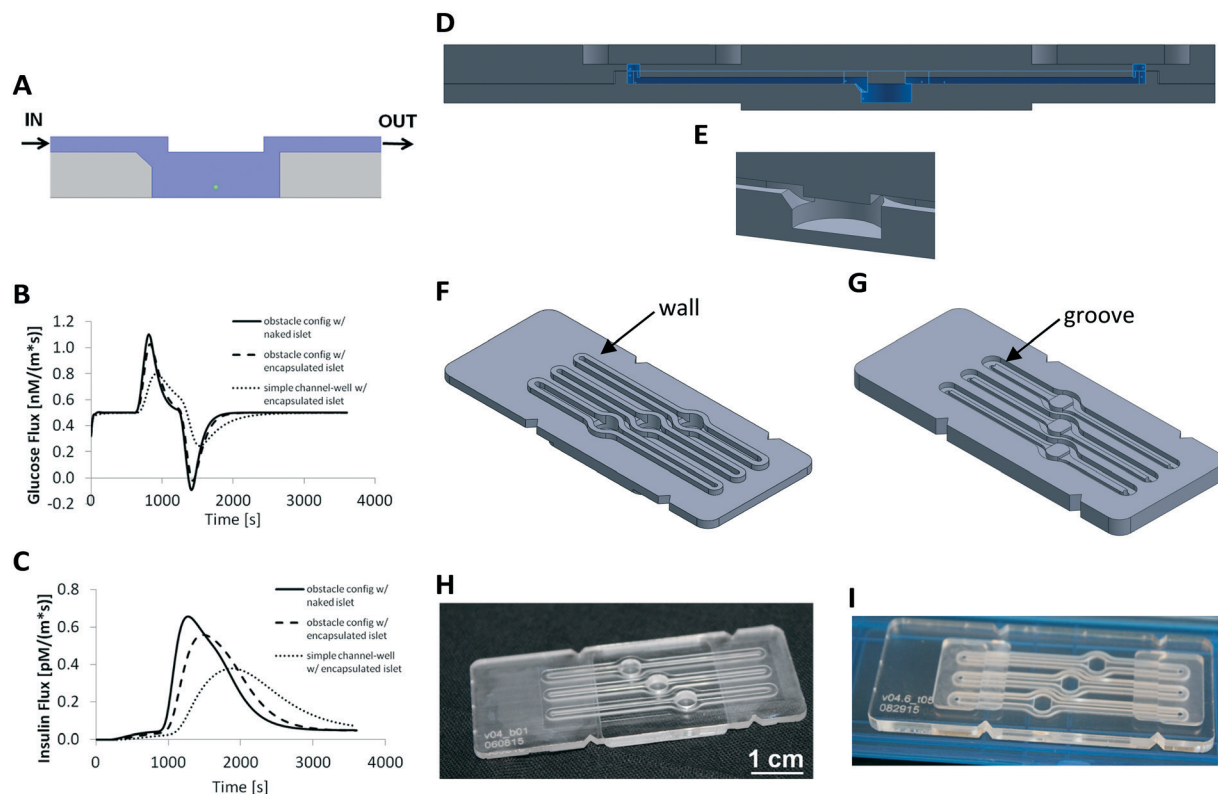
Fig. 1 Design and fabrication of the present device (FP-3W). A COMSOL 2D sketch (A) of a cross-section of the fluidic device shows the fluid volume in blue, a sample spherical islet in green (150 μm in diameter), and the device structure in grey. (B) Simulation of total glucose flux during a dynamic GSIS test, calculated at the islet boundary by the computational model[25] with the present device geometry at the boundary of a free (naked) islet (thicker line), encapsulated islet (dotted line) and on a plain geometry (no overhanging obstacle and chamfered inlet). (C) Simulation of total insulin flux during a dynamic GSIS test, calculated at the outlet of the device in the same configuration as in (B). A CAD assembly of FP-3W is shown in its cross-section (D) and in a 3D close-up of the well (E). The 3D CAD design of the bottom part (F) and top part (G) of FP-3W is presented together with the actual fabricated FP-3W bottom (H) and top (I).

practical loading and retrieval of the islets. An obstacle (0.50 mm high) was implemented to direct flow down into the islet-containing well. At the same time, a divergent inlet was used to reduce the flow velocity within the well, thus reducing the shear stress on the islet, without delaying the nutrient supply and secrotome collection, which was achieved by a 45° chamfer at the inlet of the well. Finally, a narrow well outlet (0.50 mm in width) that induces a vertical component to the velocity was employed to promote the transport of secreted insulin out of the well in a timely manner. The geometry also took into account the manufacturing accuracy by standard machining tools (25 μm in X–Y direction and 50 μm in the Z direction), and ease of handing and use. The simulated islet has a diameter of 150 μm and it was placed in the center of the well and raised 25 μm from the bottom. The latter was introduced because the calculation is 2D, therefore an islet in direct contact with the bottom surface would have prevented the solute to flow around the islet.

The profile of total glucose flux calculated on the boundary of the islet (Fig. 1B) shows more efficient islet perfusion than obtained with simple straight channel geometries. The first positive peak corresponds to the high glucose wave entering the islet (peak's FWHM is 200 s), while the second neg-

ative peak corresponds to outflux of glucose following the low glucose wave; solution transition happens in about two minutes, and the solution is completely switched in the well in about five minutes. Other systems[27] presented in literature show a higher glucose delivery resolution that can be addressed by the smaller volume of the device. The profile of insulin flux at the channel outlet (Fig. 1C) demonstrates that the configuration of choice was more effective than simple channel-well geometries, as illustrated by the presence of a sharper and narrower peak. Encapsulated islets are used for transplantation for *in vivo* experiments, and, therefore, are of high interest for researchers. For this reason, the insulin profile in the presence of an alginate capsule (100 μm thick) enveloping the islet (100 μm in diameter) was also investigated; Fig. 1B and C shows a slight response delay with respect to the naked islet. Experimental studies in this report, however, were focused on naked islets.

From 2D to 3D

After optimization of the device geometry in 2D, computational aided design (CAD) was used to assess the 3D assembly features and to program standard computer numerical

control (CNC) machines and laser cutters for parts fabrication. A two-part device (Fig. 1D) was chosen for straightforward access to the well and simple islet loading. A depressed well with chamfered inlet was included in the bottom part of the device (Fig. 1E and F); the inlet and outlet channels with the corresponding fluidic ports and the obstacle were included in the top part (Fig. 1E and G). In this design, the window above was not machined to keep it optically transparent (Fig. 1I). Instead, the bottom surface of the well was milled (Fig. 1H), but it still allowed imaging by optical inverted microscopes even with objectives of working distances less than 1 mm. The chamfer at the well inlet was filleted toward the edge of the cylindrical surfaces of the well (Fig. 1E) to uniformly fill the well during perfusion.

For ease of use, an engagement feature was included to provide a consistent alignment of the two parts when assembled and disassembled. An insert, defined as "wall", was elevated with respect to the bottom surface of the device that surrounds channels and well (Fig. 1F). A groove depressed with respect to the channel was machined on the top part of the device in order to match the wall (Fig. 1G). This depres-

sion was designed to host also an elastomeric gasket that impedes liquid leakage out of the system.

The FP-3W was furnished with three independently supplied wells. In future iterations, a higher level of multiplexing could be easily conceived. Multiple experiments or test in triplets could be performed on the current platform simultaneously. The overall dimensions (61 mm × 25 mm) and notches on the device edges were fixed to fit a commercial clamping system (Fig. 2A) that holds the two parts together and provides fluid inflow and outflow.

Fabrication

The material selected for the prototypes was optically transparent acrylic (3.15 mm thick acrylic sheet from McMaster&Carr, Elmhurst, IL). It was easy to machine and served well for optical microscopy. The device features were milled with a CNC machine (Roland MDX-540) with tool accuracy of 25 μm. The higher finishing of the bottom of the well was achieved with a smaller bit (1/64″) with 4 flutes. Machining time was 1.5 hours for each part of the device, in
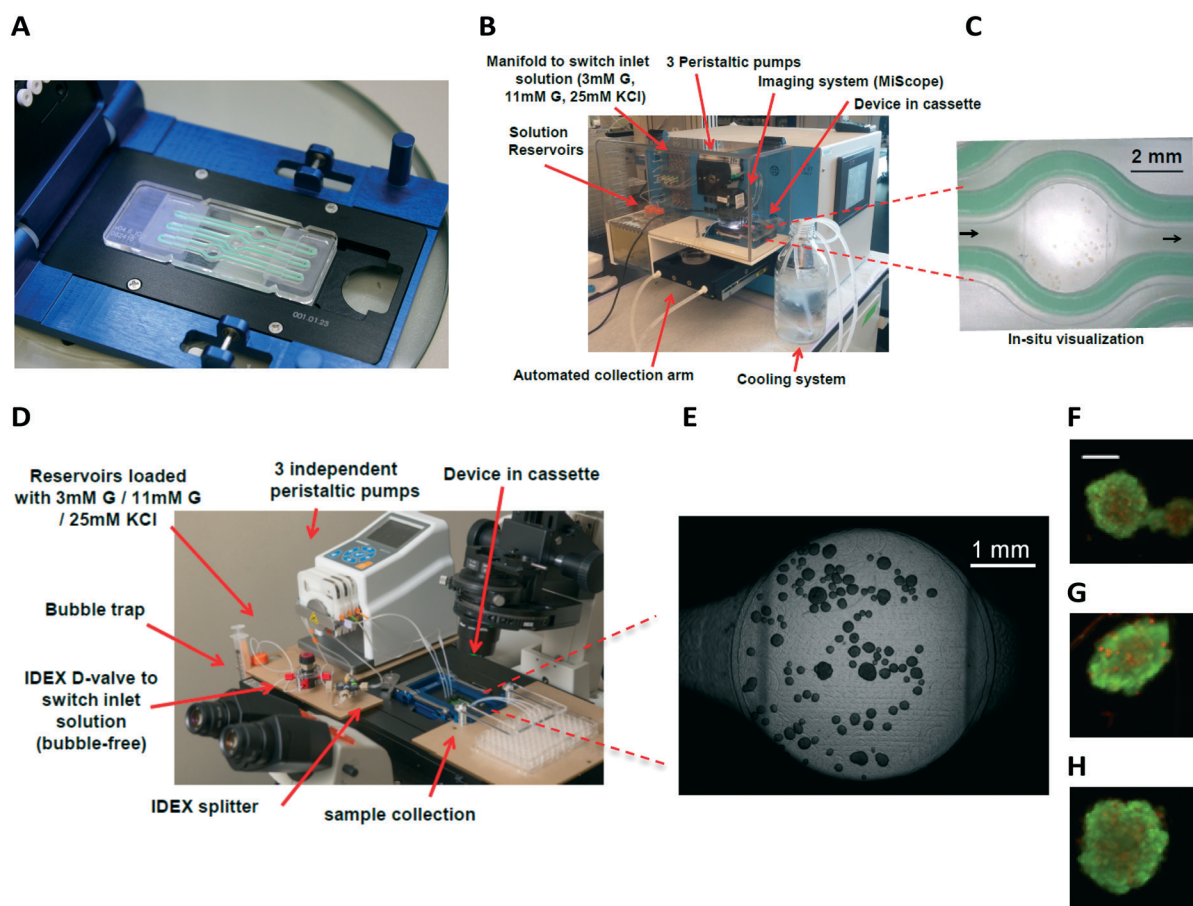

Fig. 2 Device assembly and integration in commercial tools. A cassette by Micronit Microfluidics is adopted to clamp the assembled FP-3W, where the gasket is showed in green (A). FP-3W can be integrated into a PERI4-02 Perifusion machine (B), and device operation can be monitored *via* portable microscopes (C). FP-3W can be set up on a Nikon inverted epi-fluorescent microscope (D) for higher quality imaging (E). Viability staining of human islets for each of the wells can be performed in a FP-3W after dynamic GSIS (F–H); images acquired on a Nikon epi-fluorescent inverted microscope (scale is 100 μm).

order to achieve adequate surface finishing. If a larger number of parts would be required, higher throughput fabrication methods, such as injection molding could significantly reduce processing times and cost per part.

The top part was designed to be thicker than the bottom one (Fig. 1I) to secure a homogenous gasket compression when the device was clamped. The parts were cut out of the workpiece with an Epilog 30W CO_2 Laser Engraver in order to reduce the fabrication time. Fluidic parts were clamped using a commercial cassette supplied by Micronit Microfluidics (Enschede, Netherlands). The cassette is in a standard form factor that fits SBS plate holders and enables a liquid connection through compressible perfluoroelastomer ferrules that seal PTFE tubing (1/16″ OD) at the inlet and outlet of the device.

The liquid sealing on the two-part device was provided by a custom-made gasket (500 μm thick when not compressed, Fig. 2A), which could be used at least ten times before wearing out. The gasket was based on a fast curing (<30 minutes) two-part silicone (DURASEAL 1533) that is highly resistant to chemicals, solvents and moisture. The mold was fabricated with the CNC milling machine.

Experimental set-up

Device assembly

The device assembly consisted of setting up: 1) the commercial cassette as per the instructions of the manufacturer; 2) the three gaskets in the grooves of the top part of the device; 3) the bottom part of the device into the cassette; 4) loading the islets in the pre-wetted wells; 5) aligning the two parts of the device into the cassette using the characteristic features and; 6) clamping the device down. These straightforward steps resulted in quick device assembly times (few minutes), while still ensuring robust and reproducible operation.

The quality of the assembly and the ability to allow fluid flow without any leaks, bubbles, or malfunctions was established using de-ionized water stained with colored dyes and polystyrene microbeads that resemble islet size (200 μm) and density (1.05 g cm^{-3}). The bottom surface of the well was pre-wet to avoid bubble entrapment during islet loading. Test at different flow rates confirmed that the beads were retained within the wells, even up to flow rates of 100 μL min^{-1}. In the ESI† we included a 5 minutes video (sped up 6×, frames taken every 5 seconds). The camera view (zoomed 4×) was focused on the bottom surface of one of the three wells (the round surface marks are made by the CNC machining process). The islets were simply suspended in the well. There was no drifting or floating of the islets, while only some much smaller particles (out of focus) were dragged in the direction of the flow, from left to right.

Device integration

FP-3W was designed to allow integration with a variety of research instruments, and ultimately customization to the needs of different research groups. For example, it could be integrated with the high-capacity automated perfusion system PERI4-02, sold by Biorep Inc. (Miami, FL), an instrument commonly used by islet researchers for dynamic insulin testing. PERI4-02 integrates: a) a manifold to switch among different reservoirs, as needed by the perfusion tests; b) a set of peristaltic pumps to supply up to 12 wells independently; c) a set of special macro-chambers in a vial form factor that maintain the islets during the test and; d) an automated collection arm that enables a dynamic measure of hormone secretion from the islets. The reservoirs containing the perfusion solutions and the vial chambers containing the islets could be kept at 37 °C, whilst the automated arm was kept at 4 °C to maintain the quality of the samples in the collection plate. While an elegant design, the procedure required to prepare the vial chambers that contain the islets could be cumbersome. Multiple steps and components (e.g. assembling filters and gel spheres for each vial) are involved and a certain level of experience is needed to achieve reproducible results. Alternatively, the FP-3W provides a significantly more user-friendly approach. After straightforward manual loading of islets, the clamped device was connected to the pump with tube sleeves (Fig. 2B) and ready to use. A portable imaging system (MiScope by Zarbeco) could be set up above the device to monitor the islets during the device operation (Fig. 2C).

Additionally, for added flexibility, the FP-3W could be set up directly on an inverted fluorescent microscope (Fig. 2D), which enables besides other standard imaging applications (Fig. 2E–H), the manipulation of islet physiology through light stimulation (optogenetics), whilst evaluating dynamic pancreatic islet secretory activity.

Dynamic insulin measurement

The dynamic measurement of insulin consists of stimulating the islets with glucose in a manner that permits assessment of their sensitivity to glucose and ability to secrete insulin in a dynamic manner. Further, to characterize total insulin production, a high concentration of potassium chloride is often used to depolarize the islet. Outflow samples were collected and correlated to introduction of different stimuli after an off-line measurement of insulin. The solutions to stimulate the islets were based on a 'HEPES buffer' that consists of: 125 mM NaCl, 5.9 mM KCl, 2.56 mM $CaCl_2$, 1.2 mM $MgCl_2$, 25 mM HEPES, 0.1% BSA, at pH 7.4. The low and high glucose stimulus solutions were made by adding 3 mM and 11 mM glucose, respectively, to the HEPES buffer. Islet depolarization could be achieved by adding 25 or 50 mM KCl. During dynamic GSIS, islets were perfused in the following consecutive steps: 1 hour equilibration at low glucose, 6 to 10 minutes at low glucose solution, 20 minutes at high glucose solution, 16 minutes back to low glucose, terminating eventually with 5 to 10 minutes in potassium chloride and finally for 10 minutes back to low glucose.

The PERI4-02 machine was the ideal tool to switch among solutions that stimulate the islets and to collect samples at the outlet in an automated way. After the machine was

primed, hand-picked islets were loaded into the device. Each well hosted between 10 and 60 islets. FP-3W was interfaced with the PERI4-02 machine by simply connecting the tubing of the cassette and pump *via* sleeves. A solution with low levels of glucose was flowed through the device for one hour to stabilize the islets. Flow rate was set at 50 μL min^{-1} and sampling rate was set at 2 minutes. Thus, 93 samples were collected during the whole perfusion test. Collected samples were frozen to −80 °C and insulin content measured at a later time using a standard Mouse Insulin ELISA kit (Mercodia, Uppsala, Sweden).

Viability assay

Viability assessments were performed using a Live-Dead Viability/Cytotoxicity kit (Invitrogen, Carlsbad, CA) per the instructions of the manufacturer. FP-3W allowed implementation of the protocol both in a static or dynamic mode. In static mode, the device could be disassembled and the staining solution could be added directly into the wells of the device. In dynamic mode, the staining and washing solution could be flowed through the device. Indeed, islets could be imaged directly within the device avoiding the need to move islets to a different plate just for fluorescence microscopy (Fig. 2F–H). The dynamic mode was more convenient, as a simple switch of the manifold permitted flow-through solution and staining of the islets. The cassette with the same form factor as a SBS plate could be easily accommodated on a plate holder of an epi-fluorescent microscope for image acquisition.

Optogenetic studies

The device FP-3W enabled the ability to detect light-induced somatostatin secretion in islets from transgenic mice whose delta cells expressed the light sensitive ionic channel channelrhodopsin-2 (ref. 28) (Chr2). When blue light (488 nm) excites the delta cells bearing Chr2, conformational changes in this channel allows the influx of cations depolarizing the cell membrane and triggering secretory events. It was tested whether the light stimulation of islets bearing delta cell with Chr2 induced an increase in the secretion of the delta cell main product somatostatin. The microscope blue light was used to excite two out of the three wells of FP-3W, each of them loaded with 50 islets. The fluid handling capability needed for running an islet perfusion assay could be set up directly on the microscope (Fig. 2B) with a peristaltic pump, a manual manifold, and collection plate. For the experiment 'HEPES buffer' containing 6 mM glucose was perfused throughout the device at a flow rate of 50 μl min^{-1}, while sampling rate was set at 2 min. As a positive control 25 mM of KCl was perfused for 2 min at the end of the procedure. The microscope stage was programmed to switch from one well to the next every 5 s, so that blue light could excite two wells out of three for a total of 30 s excitation during a first stimulation and 60 s for a second stimula-

tion. The third well was not excited with blue light at anytime and served as a control.

The system allowed the simultaneous stimulation of the islet with light and collection of the perfusate to evaluate the dynamic secretion of somatostatin in response to the light or KCl as positive control for delta cell secretion. Collected samples were stored at −80 °C until tested with a commercial somatostatin detection ELISA kit (Phoenix Pharmaceuticals, Burligame, CA).

Results

For direct comparison, dynamic GSIS was performed in parallel with two PERI4-02 instruments: one containing the standard vial chambers and the second featuring the FP-3W. Primary mouse islets from the same isolation were used 24 hours post-isolation. The desired number of islets, varying in size from 50 to 250 μm, were hand-picked. Two standard vials were loaded with ~100 islet equivalents (IEQs, a standard islet of 150 μm diameter[29]), and the FP-3W was manually loaded with only ~20 IEQ per well. The same stimulatory solutions were used in both experiments and prepared as explained in the experimental section. Flow rate within vial chambers for PERI4-02 was maintained at 100 μL min^{-1} with one sample collected every minute. Experiments with FP-3W were performed at a flow rate of 50 μL min^{-1} (the rate predicted by simulations to be appropriate for perfusion), with a sampling rate of one sample every two minutes. In Fig. 3A, the temporal insulin signal collected from the two PERI4-02 vial chambers is compared to each well of the FP-3W. Values are normalized to islet number (IEQ) and perfusion flow rate. Both systems were able to capture the full dynamic response of the islets, with both first phase (initial peak) and second phase (plateau) secretion observed during the high glucose stimulation phase.[30] There is strong agreement in the scale and trend of insulin secretion profiles when comparing both devices.

To demonstrate that FP-3W could be used by the larger islet research community, devices were shared with a laboratory at University of Florida for testing. Following a short training and sharing of schematics of how to connect the device to the PERI4-02 machine, islet perfusion was subsequently conducted on mouse islets 24 hours post-isolation. For this test, 50 islets were hand-picked and manually loaded into each well before clamping the device and connecting with the PERI4-02. A low-glucose solution was perfused for about 30 minutes at 100 μL minute to stabilize the islets and to confirm that the device was operating correctly (*i.e.* wells were properly filled, samples could be collected at the outlet and there were no leaks). Fig. 3B presents the insulin collected in each of the 3 individual wells of the device every minute during the stimulatory phase of the experiment, resembling the temporal insulin secretion related to each of the different stimuli (highlighted in a different gray scale). In this case, the typical biphasic insulin release during high glucose stimulation was also observed. Comparison of the
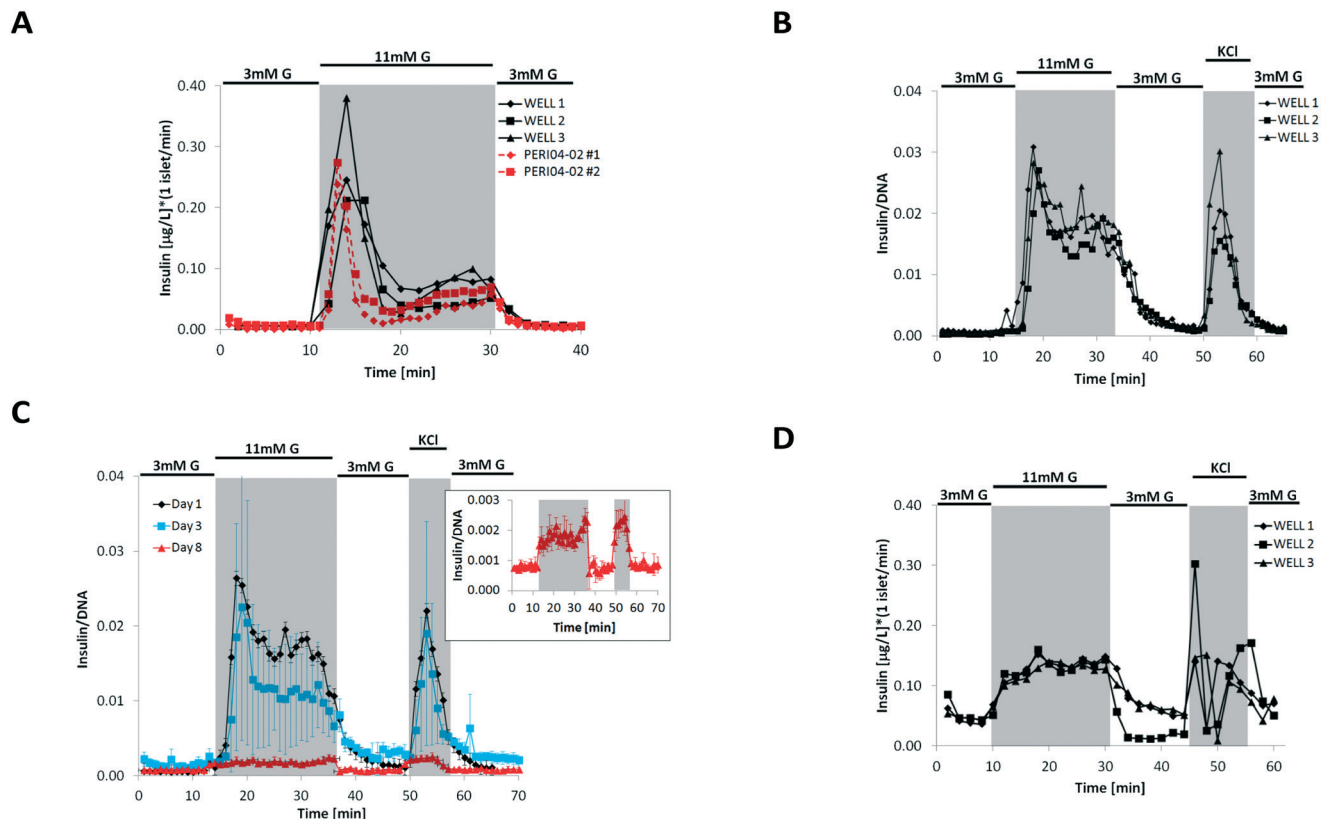
Fig. 3 Experimental results. (A) Comparison of dynamic GSIS performed in the three channels of the present device (FP-3W, solid black lines) and two standard vial chambers of the commercial PERI4-02 machine (dotted red lines) with mouse islets obtained from the same isolation. FP-3W was run at flow rate of 50 μL min^{-1} (per channel) with sampling every two minutes, while PERI4-02 vial chamber was run at 100 μL min^{-1} with sampling every minute. (B) Dynamics GSIS in mouse islets performed with FP-3W installed on a PERI4-02 platform at University of Florida. FP-3W was run at 100 μL min^{-1} (per channel) with sampling every minute. (C) Dynamic GSIS in B6 mice islets performed at day 1 (black line), 3 (blue) and 8 (red) after isolation; FP-3W was installed on a PERI4-02 and flow run at 100 μL min^{-1} (per channel) with sampling every minute. (D) Dynamic GSIS in human islets performed with FP-3W installed on a PERI4-02 platform; FP-3W was run at 50 μL min^{-1} (per channel) with sampling every two minutes.

insulin profiles for the three independent wells demonstrated synching of flow rates and stimulation, as well as insulin clearance. Minor variations in the second phase of insulin secretion were within the expected range due to the heterogeneity of the primary islets. Insulin release following KCl depolarization indicated some deviation in total insulin content between wells, although this was within the average variance observed when conducting islet perfusion using standard equipment. The time delay between the switch in inlet solution and the corresponding secreted hormone collection was due mostly to the large volume of the tubing associated with PERI4-02. The system dead volume is 600 μL (less than 100 μL is due to the device), therefore there was a delay of 6 minutes at the perfusion flow rate of 100 μL min^{-1}. Users found it convenient to work with the device when compared to standard vial chambers provided with the PERI4-02. Fewer components were involved in the assembly of the current platform, and they were large enough for easy handling. Furthermore, FP-3W could be conveniently disassembled to retrieve the islets for post-processing, such as DNA quantification for normalization. Another advantage was that the smaller device volume allowed quantification of signal from

a smaller number of islets. The optical access was found to be convenient for local inspection and imaging. Finally, the response delay was reduced because the device volume was an order of magnitude smaller than that of the PERI4-02 vial chambers (~1 mL).

Fig. 3C shows the perfusion assay after 1, 3 and 8 days in culture (in CMRL media, *i.e.* 10% FBS, 1% l glutamine, 1% penicillin streptomycin; at 37 °C and 5% CO$_2$). A new subset of B6 mice islets were loaded in each of the 3 wells and retrieved after the perfusion for DNA quantification. Fig. 3C shows the insulin profile, that is the average of the signals of the three wells. The error bar, that is ±1σ, show a large variability only at day 3, especially because the signal coming from one of the three wells was particularly low. At day 8 (showed in the insert of Fig. 3C), the released insulin was minimal but still measurable.

To translate the platform to clinically relevant assessments, a perfusion test was run with human islets (provided by the Human Islet Cell Processing Facility at the Diabetes Research Institute, University of Miami Miller School of Medicine under IRB approval for use of human tissue for research) 4 days post-isolation. To evaluate the impact of islet

loading, 25, 30, and 60 islets were manually loaded into the three wells. Fig. 3D shows the time profile of the secreted insulin, collected independently for each well and normalized to IEQ. Although the first phase of insulin release was not as defined as that seen in rodent islets, this was expected for human islet preparations. Insulin secretion, however, was elevated under high glucose, indicated responsiveness of the islets. Further, a peak of insulin release was observed under KCl stimulation, albeit with a response delay from well to well. Overall, these results demonstrated the capacity of the platform to characterize dynamic secretion of human islets, with sensitivity down to only 20 islets per well.

After sample collection, the viability assay was performed in dynamic mode as described in the experimental section. Fig. 2F–H shows examples of islets hosted in the three different wells of the device. The prevalence of dead cells (in red) was limited compared to the live cells (in green) confirming high islet viability.

Moreover, the device allowed the stimulation and perfusion of mouse islets whose delta cell expressed channelrhodopsin-2. Somatostatin content was significantly increased in samples collected right after the blue light excitation to two out of the three wells of the device ($p < 0.05$, Fig. 4A), and it was comparable with the somatostatin amount obtained in response to KCl control stimulation (time profile shown in Fig. 4B). A slight rise in somatostatin was detected for samples from the control well during the

time when the other two wells were stimulated (Fig. 4C) most likely due to background scattering, however the amount was considered not significant. Because Chr2 transgene was coupled to tomato red fluorescent protein as an expression reporter, it was possible to visualize the red fluorescent delta cells in the islets from this particular transgenic mouse (Fig. 4D). We were able to maintain the islets steady even when they are subject to shear flow (see video in ESI,† in which the islets do not show any drifting or floating).

Discussion

Since islet size[29] varies from 50 to 500 μm, fluidic platforms for assaying islet function can take advantage of much more rapid prototyping techniques (*e.g.* CNC machining) than the commonly used photolithography. Indeed, that serves better in an iterative design-prototyping-test process.

We adopted simple plastic, *i.e.* acrylic, for fabrication because it is easy to mill with standard CNC machines, it is optically clear and can be easily acquired commercially. However, acrylic is not as rigid as glass or metal; therefore strengthening features has to be integrated within the structure. We included features to conveniently align the two components of the device, and host gaskets to seal the liquid when the device was clamped. Optical access to the islets was another critical feature integrated within the design of FP-3W
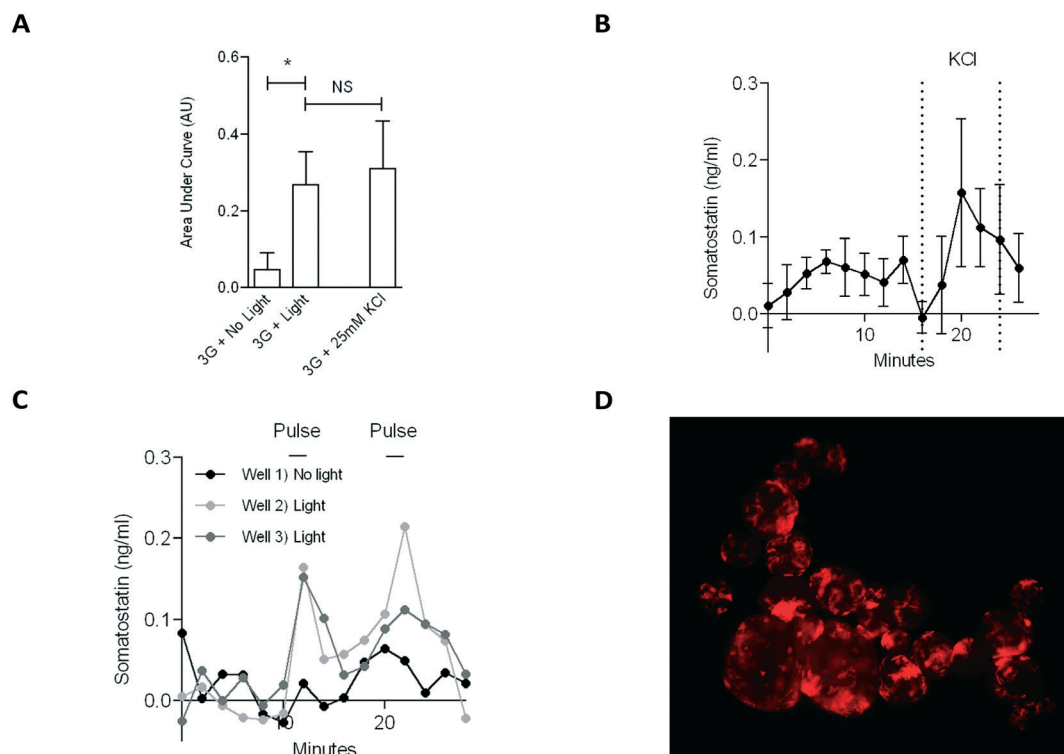

Fig. 4 Optogenetics study on delta cells. (A) Comparison of somatostatin released in each condition, calculated as cumulative signal (area under the curve), response to light is compared to the response to KCl; both anova and *t*-test have a $p < 0.05$. (B) Somatostatin response to depolarization induced by KCl stimulus, average ($\pm\sigma$) of 3 wells (no light). (C) Somatostatin time response to light stimulation in two wells out of three, third well contains the control (no light). (D) Islets expressing red fluorescent protein (RFP) show the delta cell structure.

so as to perform both qualitative and quantitative microscopy. The ability to correlate real-time imaging in parallel with standard hormone detection assays can lead to a very powerful research tool. Inverted fluorescence microscopy was possible through the milled well bottom because of its higher surface finishing and subsequent wetting that improves optical transparency.

Even if the implemented fabrication techniques were not suitable for micrometric wells, features are still small enough to reduce the dead volume to a minimum. The dead volume of the FP-3W is an order of magnitude smaller than that of standard vial chambers used in the current Biorep Perifusion machine; therefore the time delay is reduced and time resolution is improved. Moreover, FP-3W is able to operate with a smaller sample of islets, with sensitivity of perfusion confirmed for as little as 10 islets (IEQ). Thus, the resolution of the islet response is increased and more specific stimuli could be investigated (*e.g.*, drugs, toxins, immune cells, and others). This has been proved also when the insulin levels are extremely low but relative variations can still be appreciated (see perfusion at day 8 in Fig. 3C). Moreover, the high sensitivity was demonstrated by the ability to detect somatostatin. Its secretion is much less than any other hormone produced by the islet, because it is released by delta cells that are less than 10% of the total amount of cells in an islet.[31]

Further, characterization of dysfunctional islets, such as those isolated from type 1 diabetic patients, could be feasible. Indeed, using a smaller number of islets could identify characteristic phenomena that might be otherwise hidden across a large number of islets. Finally, devices that allow functional evaluation from a smaller sample size are perfectly suited for running experiments with the limited resource of human islets.

Gas bubble nucleation within fluidic devices is often unavoidable due to dissolved gas constituents of the media such nitrogen and oxygen. Moreover the device is kept at 37 °C during the perfusion test, which favors bubble nucleation. Occasionally, gas bubbles were observed; however, they were trapped on top of the well, resulting in no direct impact on the islets on the bottom of the well. Unexpectedly, these bubbles effectively lower the obstacle within the flow path, which increases the convective component of the flow at the inlet and outlet of the well. Further, they reduce the dead volume, resulting in a faster response of the device to a change in stimuli. As such, bubble formation has not been found to be a major concern in platform operation during acute assays. Moreover, sample collection is not impacted, as only 10 μL of the 100 μL sample collected is needed for ELISA analyses. Finally, the presence of bubbles inside the wells does not affect fluorescence microscopy with inverted microscopes because the bubbles are trapped on the ceiling of the well and do not obstruct the optical path. Nonetheless, we are aware of complications that bubbles could induce during a long-term culture, therefore design iterations that incorporate inline bubble traps are currently being explored. Efforts are also underway to test the platform for long term *ex vivo* culture of islets as well as high resolution imaging with integrated imaging modalities, *e.g.*, use of optical biosensors[32] for real-time detection of insulin and other hormones.

Optogenetics is finding emerging applications in diabetes research and would strongly benefit from the possibility to selectively stimulate a subset of islets while perfusing them. This unique feature of FP-3W resulted in an ideal tool for optogenetic stimulation coupled to higher temporal resolution of sample collection that enables new assays not available before. Indeed, to the best of our knowledge, this tool permitted for the first time induction of somatostatin secretion using Chr2 channels.

For organ on chip applications, this platform is amenable to both rapid and continuous perfusion of drug solutions. Hence, *in vitro* drug testing for acute and chronic exposure studies is feasible. It is also possible to recreate pathological events such as hypoxia, immune attack, and inflammation by continuous perfusion of signalling molecules such as small cytokines. More importantly, the principles of the fluidic device design, fabrication and operation can be directly extended to creating organ mimics with other *ex vivo* tissue or bioengineered organotypic cultures. While the form factor of the individual chips might differ, if they can be made to fit with similar commercial clamps, the fluidic integration would be straightforward and will pave the way for coupled organ on chip initiatives.

Conclusions

We showed that by designing geometrical features of the device from first principles-based computational modeling, it was possible to adequately perfuse the islets and allow for sample collection in a timely manner. Since manual loading and handling of the islet sample was highly desirable, we opted for a two-part device that could be sealed after islet loading. Further, disassembly of the device gave the user direct access to the islets at the end of the experiment, *e.g.* for DNA quantification. Results of the viability assay demonstrated that different assays and imaging could be performed either in line or after disassembling the device. Tests with rodent and human islets, direct comparison with existing commercial perfusion systems, and operation of the device by users from collaborating biomedical laboratories indicated that the fluidic platform is a robust, yet simple, research tool. Finally, the device proved to be an ideal platform to perform time-resolved optogenetics studies, thanks to the ability to selectively stimulate a small set of islets and still be able to detect low levels of secreted somatostatin. While sophisticated devices might serve specific needs better, if they are too complicated to use, islet biologists and pharmaceutical researchers might not implement them in their routine. We hope that our microsystem could ultimately be a powerful and practical addition to the armamentarium of diabetes researchers.

Acknowledgements

References

1 J. Buse, K. Polonsky and C. Burant, in *Williams Textbook of Endocrinology*, Elsevier Health Sciences, 2012, ch. 31, pp. 1371–1435.

2 W. Yang, T. Dall, P. Halder, P. Gallo, S. Kowal, P. Hogan and M. Petersen, *Scientific Statement American Diabetes Association*, 2013.

3 B. J. Hering, *et al.*, *Diabetes Care*, 2016, **39**, 11.

4 K. Heileman, J. Daoud, C. Hasilo, M. Gasparrini, S. Paraskevas and M. Tabrizian, *Biomicrofluidics*, 2015, **9**, 13.

5 J. G. Shackman, K. R. Reid, C. E. Dugan and R. T. Kennedy, *Anal. Bioanal. Chem.*, 2012, **402**, 7.

6 G. Orlando, P. Gianello, M. Salvatori, R. J. Stratta, S. Soker, C. Ricordi and J. Dominguez-Bendala, *Diabetes*, 2014, **63**, 1433–1444.

7 J. D. Jonhnson, *Diabetologia*, 2016, **59**, 11.

8 E. W. Esch, A. Bahinski and D. Huh, *Nat. Rev. Drug Discovery*, 2015, **14**, 248–260.

9 S. N. Bhatia and D. E. Ingber, *Nat. Biotechnol.*, 2014, **32**, 760–772.

10 M. Nourmohammadzadeh, Y. Xing, J. W. Lee, M. A. Bochenek, J. E. Mendoza-Elias, J. J. McGarrigle, E. Marchese, Y. Chun-Chieh, D. T. Eddington, J. Oberholzer and Y. Wang, *Lab Chip*, 2016, **16**, 1466–1472.

11 M. G. Roper, J. G. Shackman, G. M. Dahlgren and R. T. Kennedy, *Anal. Chem.*, 2003, **75**, 7.

12 A. F. Adewola, D. Lee, T. Harvat, J. Mohammed, D. T. Eddington, J. Oberholzer and Y. Wang, *Biomed. Microdevices*, 2010, **12**, 409–417.

13 J. V. Rocheleau, G. M. Walker, W. S. Head, O. P. McGuinness and D. W. Piston, *Proc. Natl. Acad. Sci. U. S. A.*, 2004, **101**, 12899–12903.

14 J. S. Mohammed, Y. Wang, T. A. Harvat, J. Oberholzer and D. T. Eddington, *Lab Chip*, 2009, **9**, 97–106.

15 F. R. Castiello, K. Heileman and M. Tabrizian, *Lab Chip*, 2016, **16**, 409–431.

16 S. Zheng and C. E. Mathews, *Curr. Diabetes Rep.*, 2014, **14**, 519.

17 M. Nakayama, K. M. Simmons and A. W. Michels, *Curr. Diabetes Rep.*, 2015, **15**, 113.

18 N. S. Wilcox, J. Rui, M. Hebrok and K. C. Herold, *J. Autoimmun.*, 2016, **71**, 51–58.

19 R. Lehmann-Werman, D. Neiman, H. Zemmour, J. Moss, J. Magenheim, A. Vaknin-Dembinsky, S. Rubertsson, B. Nellgård, K. Blennow, H. Zetterberg, K. Spalding, M. J. Haller, C. H. Wasserfall, D. A. Schatz, C. J. Greenbaum, C. Dorrell, M. Grompe, A. Zick, A. Hubert, M. Maoz, V. Fendrich, D. K. Bartsch, T. Golan, S. A. B. Sasson, G. Zamir, A. Razin, H. Cedar, A. M. J. Shapiro, B. Glaser, R. Shemer and Y. Dor, *Proc. Natl. Acad. Sci. U. S. A.*, 2015, 9.

20 J. L. Kopp, M. Grompe and M. Sander, *Nat. Cell Biol.*, 2016, **18**, 238–245.

21 O. Cabrera, M. C. Jacques-Silva, D. M. Berman, A. Fachado, F. Echeverri, R. Poo, A. Khan, N. S. Kenyon, C. Ricordi, P.-O. Berggren and A. Caicedo, *Cell Transplant.*, 2008, **16**, 10.

22 J. F. Dishinger, K. R. Reid and R. T. Kennedy, *Anal. Chem.*, 2009, **81**, 3119–3127.

23 D. Chen, W. Du, Y. Liu, W. Liu, A. Kuznetsov, F. E. Mendez, L. H. Philipson and R. F. Ismagilov, *Proc. Natl. Acad. Sci. U. S. A.*, 2008, **105**, 16843–16848.

24 P. N. Silva, B. J. Green, S. M. Altamentova and J. V. Rocheleau, *Lab Chip*, 2013, **13**, 4374–4384.

25 P. Buchwald, *Theor. Biol. Med. Modell.*, 2011, **8**, 20.

26 P. Buchwald, S. R. Cechin, J. D. Weaver and C. L. Stabler, *Biomed. Eng. Online*, 2015, **14**, 28.

27 X. Li, J. C. Brooks, J. Hu, K. I. Ford and C. J. Easley, *Lab Chip*, 2017, **17**, 341–349.

28 E. S. Boyden, F. Zhang, E. Bamberg, G. Nagel and K. Deisseroth, *Nat. Neurosci.*, 2005, **8**, 1263–1268.

29 P. Buchwald, X. Wang, A. Khan, A. Bernal, C. Fraker, L. Inverardi and C. Ricordi, *Cell Transplant.*, 2009, **18**, 1223–1235.

30 P. Rorsman, L. Eliasson, E. Renström, J. Gromada, S. Barg and S. Göpel, *Physiology*, 2000, **15**, 72–77.

31 O. Cabrera, D. M. Berman, N. S. Kenyon, C. Ricordi, P. O. Berggren and A. Caicedo, *Proc. Natl. Acad. Sci. U. S. A.*, 2006, **103**, 2334–2339.

32 R. Rodriguez-Diaz, R. Dando, Y. A. Huang, P. O. Berggren, S. D. Roper and A. Caicedo, *Nat. Protoc.*, 2012, 7, 1015–1023.